

Measurement of the W^+W^- Production Cross Section and Search for Anomalous $WW\gamma$ and WWZ Couplings in $p\bar{p}$ Collisions at $\sqrt{s} = 1.96$ TeV

- T. Aaltonen,²⁴ J. Adelman,¹⁴ B. Álvarez González^{v, 12} S. Amerio^{dd, 44} D. Amidei,³⁵ A. Anastassov,³⁹ A. Annovi,²⁰ J. Antos,¹⁵ G. Apolinari,¹⁸ A. Apresyan,⁴⁹ T. Arisawa,⁵⁸ A. Artikov,¹⁶ J. Asaadi,⁵⁴ W. Ashmanskas,¹⁸ A. Attal,⁴ A. Aurisano,⁵⁴ F. Azfar,⁴³ W. Badgett,¹⁸ A. Barbaro-Galtieri,²⁹ V.E. Barnes,⁴⁹ B.A. Barnett,²⁶ P. Barria^{ff, 47} P. Bartos,¹⁵ G. Bauer,³³ P.-H. Beauchemin,³⁴ F. Bedeschi,⁴⁷ D. Beecher,³¹ S. Behari,²⁶ G. Bellettini^{ee, 47} J. Bellinger,⁶⁰ D. Benjamin,¹⁷ A. Beretvas,¹⁸ A. Bhatti,⁵¹ M. Binkley,¹⁸ D. Bisello^{dd, 44} I. Bizjak^{jj, 31} R.E. Blair,² C. Blocker,⁷ B. Blumenfeld,²⁶ A. Bocci,¹⁷ A. Bodek,⁵⁰ V. Boisvert,⁵⁰ D. Bortoletto,⁴⁹ J. Boudreau,⁴⁸ A. Boveia,¹¹ B. Brau^{a, 11} A. Bridgeman,²⁵ L. Brigliadori^{cc, 6} C. Bromberg,³⁶ E. Brubaker,¹⁴ J. Budagov,¹⁶ H.S. Budd,⁵⁰ S. Budd,²⁵ K. Burkett,¹⁸ G. Busetto^{dd, 44} P. Bussey,²² A. Buzatu,³⁴ K. L. Byrum,² S. Cabrera^{x, 17} C. Calancha,³² S. Camarda,⁴ M. Campanelli,³⁶ M. Campbell,³⁵ F. Canelli^{14, 18} A. Canepa,⁴⁶ B. Carls,²⁵ D. Carlsmith,⁶⁰ R. Carosi,⁴⁷ S. Carrillo^{n, 19} S. Carron,¹⁸ B. Casal,¹² M. Casarsa,¹⁸ A. Castro^{cc, 6} P. Catastini^{ff, 47} D. Cauz,⁵⁵ V. Cavaliere^{ff, 47} M. Cavalli-Sforza,⁴ A. Cerri,²⁹ L. Cerrito^{q, 31} S.H. Chang,²⁸ Y.C. Chen,¹ M. Chertok,⁸ G. Chiarelli,⁴⁷ G. Chlachidze,¹⁸ F. Chlebana,¹⁸ K. Cho,²⁸ D. Chokheli,¹⁶ J.P. Chou,²³ K. Chung^{o, 18} W.H. Chung,⁶⁰ Y.S. Chung,⁵⁰ T. Chwalek,²⁷ C.I. Ciobanu,⁴⁵ M.A. Ciocci^{ff, 47} A. Clark,²¹ D. Clark,⁷ G. Compostella,⁴⁴ M.E. Convery,¹⁸ J. Conway,⁸ M. Corbo,⁴⁵ M. Cordelli,²⁰ C.A. Cox,⁸ D.J. Cox,⁸ F. Crescioli^{ee, 47} C. Cuena Almenar,⁶¹ J. Cuevas^{v, 12} R. Culbertson,¹⁸ J.C. Cully,³⁵ D. Dagenhart,¹⁸ M. Datta,¹⁸ T. Davies,²² P. de Barbaro,⁵⁰ S. De Cecco,⁵² A. Deisher,²⁹ G. De Lorenzo,⁴ M. Dell'Orso^{ee, 47} C. Deluca,⁴ L. Demortier,⁵¹ J. Deng^{f, 17} M. Deninno,⁶ M. d'Errico^{dd, 44} A. Di Canto^{ee, 47} G.P. di Giovanni,⁴⁵ B. Di Ruzza,⁴⁷ J.R. Dittmann,⁵ M. D'Onofrio,⁴ S. Donati^{ee, 47} P. Dong,¹⁸ T. Dorigo,⁴⁴ S. Dube,⁵³ K. Ebina,⁵⁸ A. Elagin,⁵⁴ R. Erbacher,⁸ D. Errede,²⁵ S. Errede,²⁵ N. Ershaidat^{bb, 45} R. Eusebi,⁵⁴ H.C. Fang,²⁹ S. Farrington,⁴³ W.T. Fedorko,¹⁴ R.G. Feild,⁶¹ M. Feindt,²⁷ J.P. Fernandez,³² C. Ferrazza^{gg, 47} R. Field,¹⁹ G. Flanagan^{s, 49} R. Forrest,⁸ M.J. Frank,⁵ M. Franklin,²³ J.C. Freeman,¹⁸ I. Furic,¹⁹ M. Gallinaro,⁵¹ J. Galyardt,¹³ F. Garberson,¹¹ J.E. Garcia,²¹ A.F. Garfinkel,⁴⁹ P. Garosi^{ff, 47} H. Gerberich,²⁵ D. Gerdes,³⁵ A. Gessler,²⁷ S. Giagu^{hh, 52} V. Giakoumopoulou,³ P. Giannetti,⁴⁷ K. Gibson,⁴⁸ J.L. Gimmell,⁵⁰ C.M. Ginsburg,¹⁸ N. Giokaris,³ M. Giordani^{ii, 55} P. Giromini,²⁰ M. Giunta,⁴⁷ G. Giurgiu,²⁶ V. Glagolev,¹⁶ D. Glenzinski,¹⁸ M. Gold,³⁸ N. Goldschmidt,¹⁹ A. Golossanov,¹⁸ G. Gomez,¹² G. Gomez-Ceballos,³³ M. Goncharov,³³ O. González,³² I. Gorelov,³⁸ A.T. Goshaw,¹⁷ K. Goulianatos,⁵¹ A. Gresele^{dd, 44} S. Grinstein,⁴ C. Grossi-Pilcher,¹⁴ R.C. Group,¹⁸ U. Grundler,²⁵ J. Guimaraes da Costa,²³ Z. Gunay-Unalan,³⁶ C. Haber,²⁹ S.R. Hahn,¹⁸ E. Halkiadakis,⁵³ B.-Y. Han,⁵⁰ J.Y. Han,⁵⁰ F. Happacher,²⁰ K. Hara,⁵⁶ D. Hare,⁵³ M. Hare,⁵⁷ R.F. Harr,⁵⁹ M. Hartz,⁴⁸ K. Hatakeyama,⁵ C. Hays,⁴³ M. Heck,²⁷ J. Heinrich,⁴⁶ M. Herndon,⁶⁰ J. Heuser,²⁷ S. Hewamanage,⁵ D. Hidas,⁵³ C.S. Hill^{c, 11} D. Hirschbuehl,²⁷ A. Hocker,¹⁸ S. Hou,¹ M. Houlden,³⁰ S.-C. Hsu,²⁹ R.E. Hughes,⁴⁰ M. Hurwitz,¹⁴ U. Husemann,⁶¹ M. Hussein,³⁶ J. Huston,³⁶ J. Incandela,¹¹ G. Introzzi,⁴⁷ M. Iori^{hh, 52} A. Ivanov^{p, 8} E. James,¹⁸ D. Jang,¹³ B. Jayatilaka,¹⁷ E.J. Jeon,²⁸ M.K. Jha,⁶ S. Jindariani,¹⁸ W. Johnson,⁸ M. Jones,⁴⁹ K.K. Joo,²⁸ S.Y. Jun,¹³ J.E. Jung,²⁸ T.R. Junk,¹⁸ T. Kamon,⁵⁴ D. Kar,¹⁹ P.E. Karchin,⁵⁹ Y. Kato^{m, 42} R. Kephart,¹⁸ W. Ketchum,¹⁴ J. Keung,⁴⁶ V. Khotilovich,⁵⁴ B. Kilminster,¹⁸ D.H. Kim,²⁸ H.S. Kim,²⁸ H.W. Kim,²⁸ J.E. Kim,²⁸ M.J. Kim,²⁰ S.B. Kim,²⁸ S.H. Kim,⁵⁶ Y.K. Kim,¹⁴ N. Kimura,⁵⁸ L. Kirsch,⁷ S. Klimenko,¹⁹ K. Kondo,⁵⁸ D.J. Kong,²⁸ J. Konigsberg,¹⁹ A. Korytov,¹⁹ A.V. Kotwal,¹⁷ M. Kreps,²⁷ J. Kroll,⁴⁶ D. Krop,¹⁴ N. Krumnack,⁵ M. Kruse,¹⁷ V. Krutelyov,¹¹ T. Kuhr,²⁷ N.P. Kulkarni,⁵⁹ M. Kurata,⁵⁶ S. Kwang,¹⁴ A.T. Laasanen,⁴⁹ S. Lami,⁴⁷ S. Lammel,¹⁸ M. Lancaster,³¹ R.L. Lander,⁸ K. Lannon^{u, 40} A. Lath,⁵³ G. Latino^{ff, 47} I. Lazzizzera^{dd, 44} T. LeCompte,² E. Lee,⁵⁴ H.S. Lee,¹⁴ J.S. Lee,²⁸ S.W. Lee^{w, 54} S. Leone,⁴⁷ J.D. Lewis,¹⁸ C.-J. Lin,²⁹ J. Linacre,⁴³ M. Lindgren,¹⁸ E. Lipelis,⁴⁶ A. Lister,²¹ D.O. Litvintsev,¹⁸ C. Liu,⁴⁸ T. Liu,¹⁸ N.S. Lockyer,⁴⁶ A. Loginov,⁶¹ L. Lovas,¹⁵ D. Lucchesi^{dd, 44} J. Lueck,²⁷ P. Lujan,²⁹ P. Lukens,¹⁸ G. Lungu,⁵¹ J. Lys,²⁹ R. Lysak,¹⁵ D. MacQueen,³⁴ R. Madrak,¹⁸ K. Maeshima,¹⁸ K. Makhoul,³³ P. Maksimovic,²⁶ S. Malde,⁴³ S. Malik,³¹ G. Manca^{e, 30} A. Manousakis-Katsikakis,³ F. Margaroli,⁴⁹ C. Marino,²⁷ C.P. Marino,²⁵ A. Martin,⁶¹ V. Martin^{k, 22} M. Martínez,⁴ R. Martínez-Ballarín,³² P. Mastrandrea,⁵² M. Mathis,²⁶ M.E. Mattson,⁵⁹ P. Mazzanti,⁶ K.S. McFarland,⁵⁰ P. McIntyre,⁵⁴ R. McNulty^{j, 30} A. Mehta,³⁰ P. Mehtala,²⁴ A. Menzione,⁴⁷ C. Mesropian,⁵¹ T. Miao,¹⁸ D. Mietlicki,³⁵ N. Miladinovic,⁷ R. Miller,³⁶ C. Mills,²³ M. Milnik,²⁷ A. Mitra,¹ G. Mitselmakher,¹⁹ H. Miyake,⁵⁶ S. Moed,²³ N. Moggi,⁶ M.N. Mondragon^{n, 18} C.S. Moon,²⁸ R. Moore,¹⁸ M.J. Morello,⁴⁷ J. Morlock,²⁷ P. Movilla Fernandez,¹⁸ J. Mülmenstädt,²⁹ A. Mukherjee,¹⁸ Th. Muller,²⁷ P. Murat,¹⁸ M. Mussini^{cc, 6} J. Nachtman^{o, 18} Y. Nagai,⁵⁶ J. Naganoma,⁵⁶ K. Nakamura,⁵⁶ I. Nakano,⁴¹ A. Napier,⁵⁷ J. Nett,⁶⁰

C. Neu^z,⁴⁶ M.S. Neubauer,²⁵ S. Neubauer,²⁷ J. Nielsen^g,²⁹ L. Nodulman,² M. Norman,¹⁰ O. Norniella,²⁵ E. Nurse,³¹ L. Oakes,⁴³ S.H. Oh,¹⁷ Y.D. Oh,²⁸ I. Oksuzian,¹⁹ T. Okusawa,⁴² R. Orava,²⁴ K. Osterberg,²⁴ S. Pagan Griso^{dd},⁴⁴ C. Pagliarone,⁵⁵ E. Palencia,¹⁸ V. Papadimitriou,¹⁸ A. Papaikonomou,²⁷ A.A. Paramanov,² B. Parks,⁴⁰ S. Pashapour,³⁴ J. Patrick,¹⁸ G. Paulettaⁱⁱ,⁵⁵ M. Paulini,¹³ C. Paus,³³ T. Peiffer,²⁷ D.E. Pellett,⁸ A. Penzo,⁵⁵ T.J. Phillips,¹⁷ G. Piacentino,⁴⁷ E. Pianori,⁴⁶ L. Pinera,¹⁹ K. Pitts,²⁵ C. Plager,⁹ L. Pondrom,⁶⁰ K. Potamianos,⁴⁹ O. Poukhov*,¹⁶ F. Prokoshin^y,¹⁶ A. Pronko,¹⁸ F. Ptchosⁱ,¹⁸ E. Pueschel,¹³ G. Punzi^{ee},⁴⁷ J. Pursley,⁶⁰ J. Rademacker^c,⁴³ A. Rahaman,⁴⁸ V. Ramakrishnan,⁶⁰ N. Ranjan,⁴⁹ I. Redondo,³² P. Renton,⁴³ M. Renz,²⁷ M. Rescigno,⁵² S. Richter,²⁷ F. Rimondi^{cc},⁶ L. Ristori,⁴⁷ A. Robson,²² T. Rodrigo,¹² T. Rodriguez,⁴⁶ E. Rogers,²⁵ S. Rolli,⁵⁷ R. Roser,¹⁸ M. Rossi,⁵⁵ R. Rossin,¹¹ P. Roy,³⁴ A. Ruiz,¹² J. Russ,¹³ V. Rusu,¹⁸ B. Rutherford,¹⁸ H. Saarikko,²⁴ A. Safonov,⁵⁴ W.K. Sakumoto,⁵⁰ L. Santiⁱⁱ,⁵⁵ L. Sartori,⁴⁷ K. Sato,⁵⁶ A. Savoy-Navarro,⁴⁵ P. Schlabach,¹⁸ A. Schmidt,²⁷ E.E. Schmidt,¹⁸ M.A. Schmidt,¹⁴ M.P. Schmidt*,⁶¹ M. Schmitt,³⁹ T. Schwarz,⁸ L. Scodellaro,¹² A. Scribano^{ff},⁴⁷ F. Scuri,⁴⁷ A. Sedov,⁴⁹ S. Seidel,³⁸ Y. Seiya,⁴² A. Semenov,¹⁶ L. Sexton-Kennedy,¹⁸ F. Sforza^{ee},⁴⁷ A. Sfyrla,²⁵ S.Z. Shalhout,⁵⁹ T. Shears,³⁰ P.F. Shepard,⁴⁸ M. Shimojima^t,⁵⁶ S. Shiraiishi,¹⁴ M. Shochet,¹⁴ Y. Shon,⁶⁰ I. Shreyber,³⁷ A. Simonenko,¹⁶ P. Sinervo,³⁴ A. Sisakyan,¹⁶ A.J. Slaughter,¹⁸ J. Slaunwhite,⁴⁰ K. Sliwa,⁵⁷ J.R. Smith,⁸ F.D. Snider,¹⁸ R. Snihur,³⁴ A. Soha,¹⁸ S. Somalwar,⁵³ V. Sorin,⁴ P. Squillacioti^{ff},⁴⁷ M. Stanitzki,⁶¹ R. St. Denis,²² B. Stelzer,³⁴ O. Stelzer-Chilton,³⁴ D. Stentz,³⁹ J. Strologas,³⁸ G.L. Strycker,³⁵ J.S. Suh,²⁸ A. Sukhanov,¹⁹ I. Suslov,¹⁶ A. Taffard^f,²⁵ R. Takashima,⁴¹ Y. Takeuchi,⁵⁶ R. Tanaka,⁴¹ J. Tang,¹⁴ M. Tecchio,³⁵ P.K. Teng,¹ J. Thom^h,¹⁸ J. Thome,¹³ G.A. Thompson,²⁵ E. Thomson,⁴⁶ P. Tipton,⁶¹ P. Tito-Guzmán,³² S. Tkaczyk,¹⁸ D. Toback,⁵⁴ S. Tokar,¹⁵ K. Tollefson,³⁶ T. Tomura,⁵⁶ D. Tonelli,¹⁸ S. Torre,²⁰ D. Torretta,¹⁸ P. Totaroⁱⁱ,⁵⁵ S. Tourneur,⁴⁵ M. Trovato^{gg},⁴⁷ S.-Y. Tsai,¹ Y. Tu,⁴⁶ N. Turini^{ff},⁴⁷ F. Ukegawa,⁵⁶ S. Uozumi,²⁸ N. van Remortel^b,²⁴ A. Varganov,³⁵ E. Vataga^{gg},⁴⁷ F. Vázquezⁿ,¹⁹ G. Velev,¹⁸ C. Vellidis,³ M. Vidal,³² I. Vila,¹² R. Vilar,¹² M. Vogel,³⁸ I. Volobouev^w,²⁹ G. Volpi^{ee},⁴⁷ P. Wagner,⁴⁶ R.G. Wagner,² R.L. Wagner,¹⁸ W. Wagner^{aa},²⁷ J. Wagner-Kuhr,²⁷ T. Wakisaka,⁴² R. Wallny,⁹ S.M. Wang,¹ A. Warburton,³⁴ D. Waters,³¹ M. Weinberger,⁵⁴ J. Weinelt,²⁷ W.C. Wester III,¹⁸ B. Whitehouse,⁵⁷ D. Whiteson^f,⁴⁶ A.B. Wicklund,² E. Wicklund,¹⁸ S. Wilbur,¹⁴ G. Williams,³⁴ H.H. Williams,⁴⁶ P. Wilson,¹⁸ B.L. Winer,⁴⁰ P. Wittich^h,¹⁸ S. Wolbers,¹⁸ C. Wolfe,¹⁴ H. Wolfe,⁴⁰ T. Wright,³⁵ X. Wu,²¹ F. Würthwein,¹⁰ A. Yagil,¹⁰ K. Yamamoto,⁴² J. Yamaoka,¹⁷ U.K. Yang^r,¹⁴ Y.C. Yang,²⁸ W.M. Yao,²⁹ G.P. Yeh,¹⁸ K. Yi^o,¹⁸ J. Yoh,¹⁸ K. Yorita,⁵⁸ T. Yoshida^l,⁴² G.B. Yu,¹⁷ I. Yu,²⁸ S.S. Yu,¹⁸ J.C. Yun,¹⁸ A. Zanetti,⁵⁵ Y. Zeng,¹⁷ X. Zhang,²⁵ Y. Zheng^d,⁹ and S. Zucchelli^{cc}⁶

(CDF Collaboration[†])

¹Institute of Physics, Academia Sinica, Taipei, Taiwan 11529, Republic of China

²Argonne National Laboratory, Argonne, Illinois 60439

³University of Athens, 157 71 Athens, Greece

⁴Institut de Fisica d'Altes Energies, Universitat Autònoma de Barcelona, E-08193, Bellaterra (Barcelona), Spain

⁵Baylor University, Waco, Texas 76798

⁶Istituto Nazionale di Fisica Nucleare Bologna, ^{cc}University of Bologna, I-40127 Bologna, Italy

⁷Brandeis University, Waltham, Massachusetts 02254

⁸University of California, Davis, Davis, California 95616

⁹University of California, Los Angeles, Los Angeles, California 90024

¹⁰University of California, San Diego, La Jolla, California 92093

¹¹University of California, Santa Barbara, Santa Barbara, California 93106

¹²Instituto de Fisica de Cantabria, CSIC-University of Cantabria, 39005 Santander, Spain

¹³Carnegie Mellon University, Pittsburgh, PA 15213

¹⁴Enrico Fermi Institute, University of Chicago, Chicago, Illinois 60637

¹⁵Comenius University, 842 48 Bratislava, Slovakia; Institute of Experimental Physics, 040 01 Kosice, Slovakia

¹⁶Joint Institute for Nuclear Research, RU-141980 Dubna, Russia

¹⁷Duke University, Durham, North Carolina 27708

¹⁸Fermi National Accelerator Laboratory, Batavia, Illinois 60510

¹⁹University of Florida, Gainesville, Florida 32611

²⁰Laboratori Nazionali di Frascati, Istituto Nazionale di Fisica Nucleare, I-00044 Frascati, Italy

²¹University of Geneva, CH-1211 Geneva 4, Switzerland

²²Glasgow University, Glasgow G12 8QQ, United Kingdom

²³Harvard University, Cambridge, Massachusetts 02138

²⁴Division of High Energy Physics, Department of Physics,

University of Helsinki and Helsinki Institute of Physics, FIN-00014, Helsinki, Finland

²⁵University of Illinois, Urbana, Illinois 61801

²⁶The Johns Hopkins University, Baltimore, Maryland 21218

²⁷Institut für Experimentelle Kernphysik, Karlsruhe Institute of Technology, D-76131 Karlsruhe, Germany

²⁸Center for High Energy Physics: Kyungpook National University,

Daequ 702-701, Korea; Seoul National University, Seoul 151-742,

Korea; Sungkyunkwan University, Suwon 440-746,

Korea; Korea Institute of Science and Technology Information,

Daejeon 305-806, Korea; Chonnam National University, Gwangju 500-757,

Korea; Chonbuk National University, Jeonju 561-756, Korea

²⁹Ernest Orlando Lawrence Berkeley National Laboratory, Berkeley, California 94720

³⁰University of Liverpool, Liverpool L69 7ZE, United Kingdom

³¹University College London, London WC1E 6BT, United Kingdom

³²Centro de Investigaciones Energeticas Medioambientales y Tecnologicas, E-28040 Madrid, Spain

³³Massachusetts Institute of Technology, Cambridge, Massachusetts 02139

³⁴Institute of Particle Physics: McGill University, Montréal, Québec,

Canada H3A 2T8; Simon Fraser University, Burnaby, British Columbia,

Canada V5A 1S6; University of Toronto, Toronto, Ontario,

Canada M5S 1A7; and TRIUMF, Vancouver, British Columbia, Canada V6T 2A3

³⁵University of Michigan, Ann Arbor, Michigan 48109

³⁶Michigan State University, East Lansing, Michigan 48824

³⁷Institution for Theoretical and Experimental Physics, ITEP, Moscow 117259, Russia

³⁸University of New Mexico, Albuquerque, New Mexico 87131

³⁹Northwestern University, Evanston, Illinois 60208

⁴⁰The Ohio State University, Columbus, Ohio 43210

⁴¹Okayama University, Okayama 700-8530, Japan

⁴²Osaka City University, Osaka 588, Japan

⁴³University of Oxford, Oxford OX1 3RH, United Kingdom

⁴⁴Istituto Nazionale di Fisica Nucleare, Sezione di Padova-Trento, ^{dd}University of Padova, I-35131 Padova, Italy

⁴⁵LPNHE, Université Pierre et Marie Curie/IN2P3-CNRS, UMR7585, Paris, F-75252 France

⁴⁶University of Pennsylvania, Philadelphia, Pennsylvania 19104

⁴⁷Istituto Nazionale di Fisica Nucleare Pisa, ^{ee}University of Pisa,

^{ff}University of Siena and ^{gg}Scuola Normale Superiore, I-56127 Pisa, Italy

⁴⁸University of Pittsburgh, Pittsburgh, Pennsylvania 15260

⁴⁹Purdue University, West Lafayette, Indiana 47907

⁵⁰University of Rochester, Rochester, New York 14627

⁵¹The Rockefeller University, New York, New York 10021

⁵²Istituto Nazionale di Fisica Nucleare, Sezione di Roma 1,

^{hh}Sapienza Università di Roma, I-00185 Roma, Italy

⁵³Rutgers University, Piscataway, New Jersey 08855

⁵⁴Texas A&M University, College Station, Texas 77843

⁵⁵Istituto Nazionale di Fisica Nucleare Trieste/Udine,
I-34100 Trieste, ⁱⁱUniversity of Trieste/Udine, I-33100 Udine, Italy

⁵⁶University of Tsukuba, Tsukuba, Ibaraki 305, Japan

⁵⁷Tufts University, Medford, Massachusetts 02155

⁵⁸Waseda University, Tokyo 169, Japan

⁵⁹Wayne State University, Detroit, Michigan 48201

⁶⁰University of Wisconsin, Madison, Wisconsin 53706

⁶¹Yale University, New Haven, Connecticut 06520

(Dated: September 7, 2018)

This Letter describes the current most precise measurement of the W boson pair production cross section and most sensitive test of anomalous $WW\gamma$ and WWZ couplings in $p\bar{p}$ collisions at a center-of-mass energy of 1.96 TeV. The WW candidates are reconstructed from decays containing two charged leptons and two neutrinos, where the charged leptons are either electrons or muons. Using data collected by the CDF II detector from 3.6 fb^{-1} of integrated luminosity, a total of 654 candidate events are observed with an expected background contribution of 320 ± 47 events. The measured total cross section is $\sigma(p\bar{p} \rightarrow W^+W^- + X) = 12.1 \pm 0.9 \text{ (stat)}^{+1.6}_{-1.4} \text{ (syst)} \text{ pb}$, which is in good agreement with the standard model prediction. The same data sample is used to place constraints on anomalous $WW\gamma$ and WWZ couplings.

PACS numbers: 14.70.Fm, 13.38.Be, 13.85.Qk

*Deceased

[†]With visitors from ^aUniversity of Massachusetts Amherst,

The measurement of W boson pair production is an important test of the standard model (SM) of particle physics. This process is also an essential background to understand for Higgs boson searches at particle colliders. Next-to-leading order (NLO) calculations of W^+W^- production in $p\bar{p}$ collisions at $\sqrt{s} = 1.96$ TeV predict a cross section of $\sigma^{NLO}(p\bar{p} \rightarrow W^+W^-) = 11.7 \pm 0.7$ pb [1, 2]. The presence of anomalous $WW\gamma$ and WWZ triple gauge boson couplings (TGC) [3] could be indications of new physics at a higher mass scale, and would lead to rates for W^+W^- production or kinematic distributions that differ from those predicted by the SM.

This Letter reports a measurement of the W^+W^- production cross section and limits on anomalous TGCs using a final state consisting of two oppositely charged leptons and two neutrinos in $p\bar{p}$ collision data collected by the CDF II detector from 3.6 fb^{-1} of integrated luminosity. First evidence for W boson pair production was reported by CDF using Tevatron Run I data [4]. This process was later measured with greater significance by CDF and D0 using 184 pb^{-1} and $224\text{--}252 \text{ pb}^{-1}$ respectively of integrated luminosity from Run II of the Tevatron [5, 6]. Recently, the D0 collaboration measured the W^+W^- cross section with a precision of 20% using 1.0 fb^{-1} of integrated luminosity from Run II [7]. Limits on anomalous TGCs have previously been reported by LEP experiments and the CDF and D0 collaborations [7, 8].

The cross section measurement uses a matrix element method in which the probability for each event to have been produced by several relevant SM processes is calculated. A likelihood ratio (LR) is formed from these

probabilities. The predicted shapes and normalizations of the signal and background LR distributions are used to extract the SM W^+W^- production cross section via a maximum-likelihood fit to the LR distribution observed in data. In general, the presence of anomalous TGCs will increase the number of events containing leptons with very high values of momentum transverse to the beam direction, as compared to SM expectations. Limits on anomalous TGCs are determined from the shape and normalization of the transverse momentum spectrum constructed from the highest transverse momentum lepton in the event, referred to as the leading lepton. The results are reported in the HISZ scheme, where three parameters, λ_Z , g_1^Z , and κ_γ , are used to describe all dimension-six operators which are Lorentz and $SU(2)_L \otimes U(1)_Y$ invariant and conserve C and P separately [9]. In the SM, $\lambda_Z = 0$ and $g_1^Z = \kappa_\gamma = 1$. In this Letter, Δg_1^Z and $\Delta \kappa_\gamma$ are used to denote the deviation of the g_1^Z and κ_γ parameters from their SM values. The non-SM values of the parameters λ_Z , g_1^Z , and κ_γ are functions of the invariant mass of the W^+W^- system, $\sqrt{\hat{s}}$. These results probe a larger range of values of $\sqrt{\hat{s}}$ and thus may only be qualitatively compared to the results from LEP, which were below $\sqrt{\hat{s}} = 209$ GeV. For hadron collisions, a dipole form factor for an arbitrary coupling $\alpha(\hat{s}) = \frac{\alpha_0}{(1+\hat{s}/\Lambda)^2}$ [9] is introduced to turn off the coupling at large $\sqrt{\hat{s}}$ and avoid a violation of unitarity. The form factor scale Λ is the scale of new physics.

In the CDF II detector [10], a particle's direction is characterized by the azimuthal angle ϕ and the pseudorapidity $\eta = -\ln[\tan(\theta/2)]$, where θ is the polar angle measured from the proton beam direction. The transverse energy E_T is defined as $E \sin \theta$, where E is the energy in the calorimeter towers associated with a cluster of energy deposition. Transverse momentum, p_T , is the track momentum component transverse to the beam line. The magnitude of the p_T for an electron is scaled according to the energy measured in the calorimeter. The missing transverse energy vector, \vec{E}_T , is defined as $-\sum_i E_T^i \hat{n}_T^i$, where \hat{n}_T^i is the unit vector in the transverse plane pointing from the interaction point to the energy deposition in calorimeter tower i . This is corrected for the p_T of muons, which do not deposit all of their energy in the calorimeter, and tracks which point to uninstrumented regions in the calorimeter. The scalar \cancel{E}_T is defined as $|\vec{E}_T|$. Strongly interacting partons produced in the $p\bar{p}$ collision undergo fragmentation that results in highly collimated jets of hadronic particles. Jet candidates are reconstructed using the calorimeter and are required to have $E_T > 15$ GeV and $|\eta| < 2.5$. Isolated lepton candidates are accepted out to an $|\eta|$ of 2.0 for electron candidates and $|\eta|$ of 1.0 for muon candidates.

The experimental signature for the decay $W^+W^- \rightarrow \ell^+\nu\ell^-\bar{\nu}$ is two reconstructed leptons with opposite charge and \cancel{E}_T from the neutrinos which escape undetected. In

Amherst, Massachusetts 01003, ^bUniversiteit Antwerpen, B-2610 Antwerp, Belgium, ^cUniversity of Bristol, Bristol BS8 1TL, United Kingdom, ^dChinese Academy of Sciences, Beijing 100864, China, ^eIstituto Nazionale di Fisica Nucleare, Sezione di Cagliari, 09042 Monserrato (Cagliari), Italy, ^fUniversity of California Irvine, Irvine, CA 92697, ^gUniversity of California Santa Cruz, Santa Cruz, CA 95064, ^hCornell University, Ithaca, NY 14853, ⁱUniversity of Cyprus, Nicosia CY-1678, Cyprus, ^jUniversity College Dublin, Dublin 4, Ireland, ^kUniversity of Edinburgh, Edinburgh EH9 3JZ, United Kingdom, ^lUniversity of Fukui, Fukui City, Fukui Prefecture, Japan 910-0017 ^mKinki University, Higashiosaka City, Japan 577-8502 ⁿUniversidad Iberoamericana, Mexico D.F., Mexico, ^oUniversity of Iowa, Iowa City, IA 52242, ^pKansas State University, Manhattan, KS 66506 ^qQueen Mary, University of London, London, E1 4NS, England, ^rUniversity of Manchester, Manchester M13 9PL, England, ^sMuons, Inc., Batavia, IL 60510, ^tNagasaki Institute of Applied Science, Nagasaki, Japan, ^uUniversity of Notre Dame, Notre Dame, IN 46556, ^vUniversity de Oviedo, E-33007 Oviedo, Spain, ^wTexas Tech University, Lubbock, TX 79609, ^xIFIC(CSIC-Universitat de Valencia), 56071 Valencia, Spain, ^yUniversidad Tecnica Federico Santa Maria, 110v Valparaiso, Chile, ^zUniversity of Virginia, Charlottesville, VA 22906 ^{aa}Bergische Universitat Wuppertal, 42097 Wuppertal, Germany, ^{bb}Yarmouk University, Irbid 211-63, Jordan ^{jj}On leave from J. Stefan Institute, Ljubljana, Slovenia,

this Letter, ℓ refers to an electron or muon. Additional signal acceptance ($\sim 12\%$) is obtained from cases where one or both W bosons decay to a tau lepton which subsequently decays to an electron or muon. There are several SM processes which result in a similar final state to W^+W^- and are therefore backgrounds in this measurement. These are other diboson production (WZ , ZZ) and top-quark pair production ($t\bar{t}$). It is also possible to observe apparent \cancel{E}_T arising from the mismeasurement of lepton energy, lepton momentum, or the hadronic part of the final state. Drell-Yan ($Z/\gamma^* \rightarrow \ell^+\ell^-$) events have no neutrinos in the final state, but due to large production rates enter the W^+W^- candidate sample via mismeasurements. A third source of background is events in which a final-state particle is misidentified. These are W +jets and $W\gamma$ production, where the W boson decays leptonically and a jet is reconstructed as a lepton candidate or the γ converts in the detector material and is reconstructed as an electron.

Events containing two oppositely charged lepton candidates are selected from the data sample. The online event triggering and selection of lepton candidates are identical to those used in the search for SM Higgs bosons decaying to two W bosons at CDF [11]. The leading-lepton p_T is required to be above 20 GeV/ c to satisfy the trigger requirements, while the second lepton is allowed to have a p_T as low as 10 GeV/ c . The requirement is also made that events contain no jet candidates, which significantly reduces $t\bar{t}$ background. A variant of \cancel{E}_T used in selecting candidate events is defined as $\cancel{E}_{T,rel} = \cancel{E}_T \sin \Delta\phi(\cancel{E}_T, \ell)$ when $\Delta\phi(\cancel{E}_T, \ell) \leq \frac{\pi}{2}$, where $\Delta\phi(\cancel{E}_T, \ell)$ is the azimuthal separation between the \cancel{E}_T and the momentum vector of the nearest lepton candidate. If $\Delta\phi(\cancel{E}_T, \ell) > \frac{\pi}{2}$, then $\cancel{E}_{T,rel} = \cancel{E}_T$. The $\cancel{E}_{T,rel}$ variable is designed to reject events where the apparent \cancel{E}_T arises from the mismeasurement of lepton energy or momentum, and is required to be above 25 GeV to reduce the otherwise large Drell-Yan contamination. This requirement is lowered to 15 GeV for electron-muon events where contributions from Drell-Yan are inherently smaller. The $W\gamma$ and heavy-flavor ($J/\psi, \Upsilon$) backgrounds are reduced by requiring that the invariant mass of the lepton pair be greater than 16 GeV/ c^2 .

With the exception of the W +1-jet background, the acceptance and kinematic properties of the signal and background processes are determined by simulation. Events from W^+W^- are simulated at NLO using the MC@NLO generator [2]. The $t\bar{t}$, WZ , ZZ , and Drell-Yan backgrounds are simulated with the PYTHIA generator [12]. The $W\gamma$ background is determined using the generator described in Ref. [13]. The response of the CDF II detector is modelled with a GEANT-3-based simulation [14]. The expected yields for each process are normalized to the cross sections calculated at partial next-to next-to-leading order ($t\bar{t}$ [15]), NLO (W^+W^- [1, 2],

TABLE I: Expected number of signal (W^+W^-) and background events along with the total number of expected and observed events in the data. Uncertainties include all systematic uncertainties described in the text.

Process	Events
Z/γ^* (Drell-Yan)	79.8 ± 18.4
WZ	13.8 ± 1.9
$W\gamma$	91.7 ± 24.8
$W + 1\text{-jet}$	112.7 ± 31.2
ZZ	20.7 ± 2.8
$t\bar{t}$	1.3 ± 0.2
Total Background	320.0 ± 46.8
W^+W^-	317.6 ± 43.8
Total Expected	637.6 ± 73.0
Data	654

WZ and ZZ [1]), or leading-order with estimated higher-order corrections ($W\gamma$ [13] and Drell-Yan [16]). Efficiency corrections for the simulated detector response to lepton candidates are determined using samples of observed $Z \rightarrow \ell^+\ell^-$ events. The $W + 1\text{-jet}$ background is calculated using the probability, measured in independent jet-triggered data samples, that a hadronic jet will be reconstructed as a lepton candidate. These probabilities are applied to the jet in the $W + 1\text{-jet}$ data sample to estimate the number of such events which will pass the full lepton identification and signal selection criteria. The expected signal and background contributions are given in Table I along with the observed number of events.

The dominant systematic uncertainties on the estimated contributions come from the luminosity measurement (6%) [17] and the simulated acceptances of the signal and background processes. The acceptance uncertainty due to the parton distribution function modeling ranges from 1.9% to 4.1% for the different processes. A 10% uncertainty is assigned to all simulated processes for the kinematic differences between leading-order and higher-order calculations, based on the difference in acceptance of W^+W^- events simulated at leading-order and NLO using the PYTHIA and MC@NLO generators respectively. This uncertainty is reduced to 5% for the W^+W^- signal, which is simulated at NLO. The cross section uncertainties are 6% on diboson production, 10% on $t\bar{t}$ and $W\gamma$ production, and 5% on Drell-Yan production. A 21% uncertainty is included for the Drell-Yan background to account for the mismodeling of \cancel{E}_T and jet production rates. Systematic uncertainties of 20% and 27% are assigned to the $W\gamma$ and $W + 1\text{-jet}$ background estimates, respectively, due to uncertainties in the modeling of the photon conversions and misidentification of a jet as a lepton. Uncertainties on the modeling of jets accounts for 2% to 4% and lepton identification and trigger efficiencies range from 1% to 7%.

For each event passing the signal selection criteria, four

matrix-element-based event probabilities are calculated corresponding to the production and decay processes $W^+W^- \rightarrow \ell^+\nu\ell^-\bar{\nu}$, $ZZ \rightarrow \ell^+\ell^-\nu\bar{\nu}$, $W + 1\text{-jet} \rightarrow \ell\nu + 1\text{-jet}$, and $W\gamma \rightarrow \ell\nu + \gamma$. In the latter two processes, the jet or γ is assumed to have been reconstructed as a charged lepton candidate. The event probability for a process X is given by

$$P_X(\vec{x}) = \frac{1}{\langle\sigma\rangle} \int \frac{d\sigma(\vec{y})}{d\vec{y}} \epsilon(\vec{y}) G(\vec{x}, \vec{y}) d\vec{y} \quad (1)$$

where \vec{x} represents the observed lepton momenta and \vec{E}_T vectors, $G(\vec{x}, \vec{y})$ is a transfer function representing the detector resolution, and $\epsilon(\vec{y})$ is an efficiency function parametrized by η which quantifies the probability for a particle to be reconstructed as a lepton. The differential cross section $\frac{d\sigma(\vec{y})}{d\vec{y}}$ is calculated using leading-order matrix elements from the MCFM program [1] and integrated over all possible true values of the final state particle 4-vectors \vec{y} . The normalization factor $\langle\sigma\rangle$ is determined from the leading-order cross section and detector acceptance for each process. These event probabilities are combined into a likelihood ratio

$$LR_{WW} = \frac{P_{WW}}{P_{WW} + \sum_j k_j P_j}, \quad (2)$$

where $j = \{ZZ, W + 1\text{-jet}, W\gamma\}$ and k_j is the relative fraction of the expected number of events for the j -th process such that $\sum_j k_j = 1$. The templates of the LR_{WW} distribution are created for signal and each background process given in Table I.

A binned maximum likelihood is used to extract the W^+W^- production cross section from the shape and normalization of the LR_{WW} templates. The likelihood is formed from the Poisson probabilities of observing n_i events in the i -th bin when μ_i are expected. Variations corresponding to the systematic uncertainties described previously are included as normalization parameters for signal and background, constrained by Gaussian terms. The likelihood is given by

$$\mathcal{L} = \left(\prod_i \frac{\mu_i^{n_i} e^{-\mu_i}}{n_i!} \right) \cdot \prod_c e^{-\frac{s_c^2}{2}} \quad (3)$$

where

$$\mu_i = \sum_k \alpha_k \left[\prod_c (1 + f_k^c S_c) \right] (N_k^{Exp})_i, \quad (4)$$

f_k^c is the fractional uncertainty for the process k due to the systematic c , and S_c is a floating parameter associated with the systematic uncertainty c . The correlations of systematic uncertainties between processes are accounted for in the definition of μ_i . The expected number of events from process k in the i -th bin is given by $(N_k^{Exp})_i$. The parameter α_k is an overall normalization parameter for process k and is fixed to unity

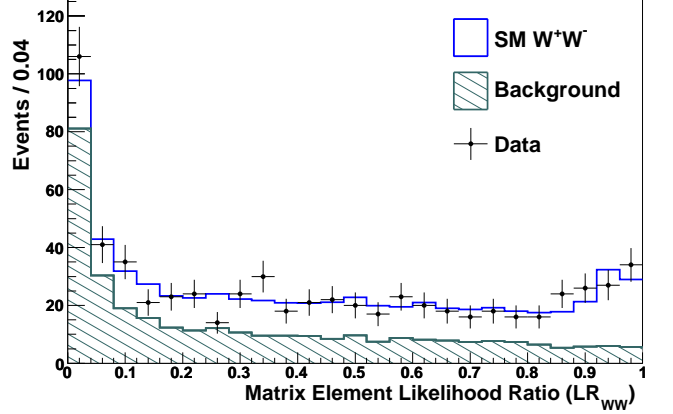


FIG. 1: The LR_{WW} distributions for the signal (W^+W^-) and background processes after a maximum likelihood fit to the data.

for all processes other than W^+W^- , for which it is freely floating. The likelihood is maximized with respect to the systematic parameters S_c and α_{WW} using the MINUIT program [18]. The W^+W^- cross section is then given by the fitted value of α_{WW} multiplied by $\sigma^{NLO}(pp \rightarrow W^+W^-)$. This method gives a measured value for the W^+W^- production cross section of $\sigma(pp \rightarrow W^+W^- + X) = 12.1 \pm 0.9 \text{ (stat)} \pm 1.6 \text{ (syst)} \text{ pb}$. The fit to the data of the signal and sum of the individually fitted background templates is shown in Fig. 1.

The likelihood of the observed leading-lepton p_T distribution is used to set limits on anomalous TGC values. The robustness of the leading-lepton p_T distribution has been verified using the same lepton selection in several non-overlapping final state kinematic regions. The response of the detector to events with different coupling constants is simulated for six points in the parameter space near the existing limits [8]. The efficiency multiplied by acceptance as a function of the leading-lepton p_T is taken to be the average of the values measured in these samples. The uncertainty is taken to be the maximum variation among these samples and ranges from 7% at low p_T to 50% at high p_T . This p_T -dependent efficiency is applied to the NLO generator-level distributions produced by the MCFM program [1] to predict the leading-lepton p_T spectrum for the coupling values considered, as shown in Fig. 2.

Each of the likelihoods $\mathcal{L}(\lambda_Z)$, $\mathcal{L}(\Delta g_1^Z)$, and $\mathcal{L}(\Delta \kappa_\gamma)$ are computed as the product over all bins in the leading-lepton p_T distribution of the Poisson probability of each bin given the model, and 95% confidence levels are set where $(-2 \ln \mathcal{L}) - (-2 \ln \mathcal{L}_{min}) = (1.96)^2$. The systematic uncertainties include all those described for the W^+W^- cross section and the additional p_T -dependent uncertainty on the efficiency described previously. Systematic uncertainties are implemented by simultaneously applying all variations which reduce the sensitivity. The

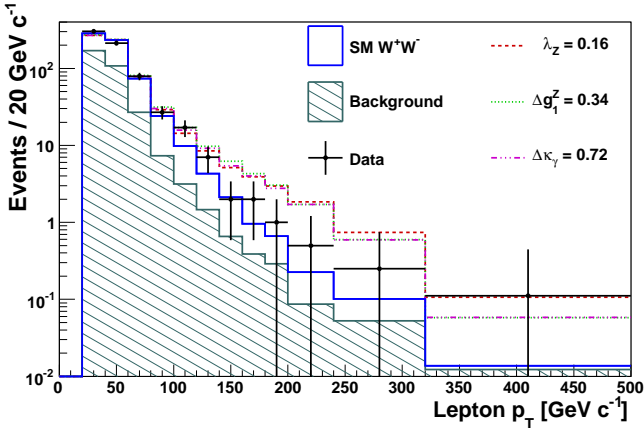


FIG. 2: Leading-lepton p_T distribution for data compared to the SM expectation. Also shown is how the expectation would be modified by anomalous couplings near the observed limits.

TABLE II: Expected and observed limits on anomalous TGCs. For each coupling limit set, the two other couplings are fixed at their SM values. Values of the couplings outside of the given observed range are excluded at the 95% confidence level.

	Λ (TeV)	λ_Z	Δg_1^Z	$\Delta \kappa_\gamma$
Expected	1.5	(-0.05,0.07)	(-0.09,0.17)	(-0.23,0.31)
Observed	1.5	(-0.16,0.16)	(-0.24,0.34)	(-0.63,0.72)
Expected	2.0	(-0.05,0.06)	(-0.08,0.15)	(-0.20,0.27)
Observed	2.0	(-0.14,0.15)	(-0.22,0.30)	(-0.57,0.65)

observed 95% confidence limits, shown in Table II, are weaker than expected. The probability of observing these limits in the presence of only standard model W^+W^- production ranges from 7.1% to 7.6% depending on the coupling constants ($\lambda_Z, g_1^Z, \kappa_\gamma$).

In summary, the W^+W^- production cross section has been measured in $p\bar{p}$ collisions at $\sqrt{s} = 1.96$ TeV from reconstructed events in the dilepton final state using a likelihood ratio formed from matrix-element-based event probabilities. This result is the most precise measurement at this energy with an overall uncertainty of less than 15%. The same event sample is also used to perform the most sensitive probe to date at this energy of anomalous WWZ and $WW\gamma$ couplings. The leading-lepton p_T distribution of the sample is found to be in moderate agreement with the SM expectation and used to place limits on anomalous triple gauge couplings.

We thank the Fermilab staff and the technical staffs of the participating institutions for their vital contributions. This work was supported by the U.S. Department of Energy and National Science Foundation; the Italian Istituto Nazionale di Fisica Nucleare; the Ministry of Education, Culture, Sports, Science and Technology of Japan; the Natural Sciences and Engineering Research

Council of Canada; the National Science Council of the Republic of China; the Swiss National Science Foundation; the A.P. Sloan Foundation; the Bundesministerium für Bildung und Forschung, Germany; the World Class University Program, the National Research Foundation of Korea; the Science and Technology Facilities Council and the Royal Society, UK; the Institut National de Physique Nucléaire et Physique des Particules/CNRS; the Russian Foundation for Basic Research; the Ministerio de Ciencia e Innovación, and Programa Consolider-Ingenio 2010, Spain; the Slovak R&D Agency; and the Academy of Finland.

- [1] J. M. Campbell and R. K. Ellis, Phys. Rev. D **60**, 113006 (1999).
- [2] S. Frixione and B. R. Webber, J. High Energy Phys. 06 (2002) 029.
- [3] J. Ellison and J. Wudka, Ann. Rev. Nucl. Part. Sci. **48**, 33 (1998).
- [4] F. Abe *et al.* (CDF Collaboration), Phys. Rev. Lett. **78**, 4536 (1997).
- [5] D. E. Acosta *et al.* (CDF Collaboration), Phys. Rev. Lett. **94**, 211801 (2005).
- [6] V. M. Abazov *et al.* (D0 Collaboration), Phys. Rev. Lett. **94**, 151801 (2005) [Erratum-ibid. **100**, 139901 (2008)].
- [7] V. M. Abazov *et al.* (D0 Collaboration), Phys. Rev. Lett. (to be published) [arXiv:0904.0673].
- [8] J. Abdallah *et al.* (DELPHI Collaboration), Eur. Phys. J. C **54**, 345 (2008); S. Schael *et al.* (ALEPH Collaboration), Phys. Lett. B **614**, 7 (2005); P. Achard *et al.* (L3 Collaboration), Phys. Lett. B **586**, 151 (2004); G. Abbiendi *et al.* (OPAL Collaboration), Eur. Phys. J. C **33**, 463 (2004); V. M. Abazov *et al.* (D0 Collaboration), Phys. Rev. D **74**, 057101 (2006); T. Aaltonen *et al.* (CDF Collaboration), Phys. Rev. D **76**, 111103 (2007).
- [9] K. Hagiwara, S. Ishihara, R. Szalapski, and D. Zeppenfeld, Phys. Rev. D **48**, 2182 (1993).
- [10] A. Abulencia *et al.* (CDF Collaboration), J. Phys. G **34**, 2457 (2007).
- [11] T. Aaltonen *et al.* (CDF Collaboration), Phys. Rev. Lett. **102**, 021802 (2009).
- [12] T. Sjostrand, S. Mrenna, and P. Skands, J. High Energy Phys. 05 (2006) 026.
- [13] U. Baur, T. Han, and J. Ohnemus, Phys. Rev. D **57**, 2823 (1998).
- [14] R. Brun, R. Hagelberg, M. Hansroul, and J. C. Lassalle, version 3.15, CERN-DD-78-2-REV.
- [15] S. Moch and P. Uwer, Nucl. Phys. Proc. Suppl. **183**, 75 (2008).
- [16] C. Anastasiou, L. J. Dixon, K. Melnikov, and F. Petriello, Phys. Rev. D **69**, 094008 (2004).
- [17] D. Acosta *et al.*, Nucl. Instrum. Methods Phys. Res., Sect. A **494**, 57 (2002).
- [18] F. James and M. Roos, Comput. Phys. Commun. **10**, 343 (1975).